



Published in final edited form as:

Head Neck. 2015 March ; 37(3): 317–326. doi:10.1002/hed.23600.

Cancer stem cells mediate tumorigenesis and metastasis in head and neck squamous cell carcinoma

Steven B. Chinn, MD¹, Owen A. Darr, MD¹, John H. Owen, MS¹, Emily Bellile, MS², Jonathan B. Mchugh, MD³, Matthew E. Spector, MD¹, Silvana M. Papagerakis, MD, PhD¹, Douglas B. Chepeha, MD¹, Carol R. Bradford, MD¹, Thomas E. Carey, PhD¹, and Mark E. P. Prince, MD¹

¹University of Michigan Department of Otolaryngology – Head and Neck Surgery, Ann Arbor, MI 48103; U.S.A

²University of Michigan Comprehensive Cancer Center Biostatistics Unit, Ann Arbor, MI 48103; U.S.A

³University of Michigan Department of Pathology, Ann Arbor, MI 48103; U.S.A

Abstract

Background—Cancer stem cells (CSC) represent a subpopulation of cells responsible for tumor growth. Their role in head and neck squamous cell carcinoma (HNSCC) tumorigenesis and metastasis remains uncertain.

Methods—Wound healing and an orthotopic animal model were used to study cells expressing the CSC phenotype (CD44^{high} and ALDH+) and assess mobility, tumorigenesis and metastasis. A prospective collection of 40 patient-derived primary HNSCC specimens were analyzed for CSC-proportion compared to clinical variables.

Results—CSC exhibited significantly faster wound closure and greater tumorigenesis and regional metastasis in-vivo than non-CSC. In primary patient tumors, size and advanced stage were correlated with elevated proportion of CSC, however not with survival.

Conclusion—HNSCC CSC mediate tumorigenesis and regional metastasis in-vivo. In primary patient tumors, CSC-proportion was associated with tumor size and stage, but not with metastatic spread or survival. CSC burden alone may only represent a minor variable in understanding CSC and metastasis.

Index Words

Cancer stem cells; CD44; Head and neck squamous cell carcinoma; metastasis; animal model

Corresponding author: Mark E. Prince, MD (mepp@med.umich.edu), (734)936-9178 (phone), (734)232-0810 (fax) Department of Otolaryngology – Head and Neck Surgery, University of Michigan, 1500 E. Medical Center Dr., Ann Arbor, MI, 48103.

Conflicts of interest: The authors disclose no potential conflicts of interest.

✉ This work was presented at the 8th International Conference on Head and Neck Cancer, Toronto, Ontario, July 2012.

We attest that neither the submitted manuscript nor any similar manuscripts is under consideration, in press, or published elsewhere.

Introduction

In the stochastic model of tumorigenesis, all cancer cells in a tumor population are capable of initiating tumor growth. The cancer stem cell (CSC) theory of tumorigenesis has recently gained popularity due to identification of a rare subset of cells, CSC, with the ability for self-renewal, regeneration of a heterogeneous tumor cell population and the ability to initiate tumors in vivo. The CSC theory holds that this subpopulation of cells are responsible for tumor growth and spread, whereas non-CSC have limited capacity for regeneration of progeny or the ability to recapitulate a tumor.¹

Head and neck squamous cell cancer (HNSCC) affects over 40,000 Americans with 11,000 dying annually.² Regional lymphatic metastasis predisposes patients to the development of distant metastasis, effectively reducing survival rates by 50%.³⁻⁶ Despite advances in treatment, overall survival remains static.² Regional and distant metastases make up a considerable proportion of the treatment failures.⁶ It is important to study factors associated with cancer spread to develop more effective diagnostic techniques and to identify therapeutic targets. Subpopulations of tumor cells with highly tumorigenic behavior can be identified in HNSCC based on the cellular markers CD44 and aldehyde dehydrogenase (ALDH).⁷⁻¹¹

Cancer stem cells have been identified in solid tumors, including breast, prostate and pancreatic carcinoma.¹¹⁻¹³ We have previously demonstrated that a subset of HNSCC cancer cells that express CD44 and ALDH have increased self-renewal, tumorigenicity, and the ability to recapitulate a heterogeneous tumor compared to cells without these markers in a flank injection mouse model.^{8,9} Cancer cells without these markers had limited or no tumorigenic potential. Additional work using a mouse tail vein injection model of CSC-mediated metastasis demonstrated that HNSCC cells expressing CD44^{high} and ALDH+ have a greater capacity to colonize the lungs compared to CD44^{low} and ALDH- tumor cells which rarely if ever lead to successful lung colonization.¹⁴ In addition, in-vitro experiments have shown that HNSCC CSC have increased motility and invasive characteristics in vitro compared to non-CSC.^{14,15} However, spontaneous metastasis from tumors initiated by head and neck CSC has not been shown. CSC may play a key role in metastasis and may serve as a novel target for therapy. Cancer stem cells are thought to be slowly replicating cells that have innate chemotherapy and radiation resistance mechanisms. That behavior is a plausible mechanism for treatment failures.^{12,16} Development of a physiologic model of metastasis using cancer stem cells is vital to demonstrate the role of CSC in metastasis and understand the mechanisms of metastasis. More importantly such a model can be used to develop novel strategies towards cancer therapy. In this paper, we will test the hypotheses that (i) CSC have a greater migratory rate compared to non-CSC in-vitro, (ii) have a greater capacity for tumorigenesis and spontaneous metastasis using an orthotopic tip of tongue mouse model, and (iii) CSC enrichment is associated with metastasis and outcome.

Materials and Methods

Patient data and tumor collection

Approval for use of Patient data and specimen collection was approved by the University of Michigan's Institutional Review Board and all patients signed written informed consent for the study as part of the University of Michigan Head and Neck S.P.O.R.E (Specialized Program of Research Excellence). Forty HNSCC patients were prospectively collected from 2007-2012 (mean age 57.5-years; M:F 25:15; median follow-up 0.8 years). Primary tumors (31 oral cavity, 8 laryngeal, 1 oropharynx) were harvested directly from tumor resection specimens. Tumor specimens were taken directly from the operating room and placed in HICCS 2% solution with amphotericin-B. Tumors were then cut into fine pieces with a scalpel and subjected to 2 hours of digestion with Collagenase-Hyaluronadase enzyme. Specimens were then placed into cell culture flasks with 10% DMEM and left undisturbed for 48 hours in a cell culture incubator. Cells were sorted by flow cytometry for CD44 expression. Tumor CSC enrichment was determined based on percentage of tumor specimen cells expressing high levels (top 1%) of CD44 based on flow. CD44 expression percentage quartiles were then identified to categorize tumor specimens for analysis. CSC enrichment and clinical covariates (T- and N-classification, AJCC stage, age, tobacco use, perineural invasion (PNI), distant metastasis (DM), tumor size, and tumor depth) were analyzed. Kaplan-Meier survival statistics were used to evaluate overall survival (OS), disease-specific survival (DSS) and disease free interval (DFI).

Cell lines and cell culture

UM-SCC-47 and UM-SCC-103 are well-established HNSCC cell lines derived from advanced stage oral cavity squamous cell carcinomas.^{17,18} Both cell lines were transfected with a luciferase cassette (luc+) for bioluminescence imaging (BLI), and were grown as previously described to 70-80% confluency, trypsinized, and sorted by flow cytometry for injection or plated for wound healing assays.¹⁴

Flow Cytometry

CSC and non-CSC were identified and sorted by flow cytometry based on cellular expression patterns of CD44 and ALDH as reported previously.^{7-9,14} ALDH activity was identified in the UM-SCC-47-luc+ and UM-SCC-103-luc+ cancer cell line using the ALDEFLUOR substrate in accord with the manufacturer's protocol (StemCo Biomedical, Durham, NC). Specimens being analyzed for ALDH activity were then counterstained with anti-CD44 (allophycocyanin [APC] conjugated; BD Pharmingen, San Diego, CA) at the appropriate dilution. Nonviable cells are eliminated using 4',6-diamidino-2-phenylindole (DAPI; BD Pharmingen). The specific flow cytometry gates for ALDH-positive cells were set using a control sample of isolated tumor cells in which ALDH activity was inhibited with diethylamino-benzaldehyde (DEAB). Cells expressing CD44 were identified using a fluorescent conjugated anti-CD44 antibody (allophycocyanin-conjugated, mouse antihuman, clone G44-26; BD Pharmingen, San Diego, California) at a 1:50 dilution for 15 to 20 minutes. Subsequent flow cytometry runs were used to identify populations of cells with positive aldehyde dehydrogenase activity (ALDH+), negative ALDH activity (ALDH-) (Supplemental Figure 1A and 1B) and cells that express high levels of CD44 (CD44^{high}) and

low levels of CD44 (CD44^{low}). (Supplemental Figure 1C and 1D) For double sorts using both CD44 and ALDH, CD44 expression was identified first followed by subsequent ALDH activity. Cells with CD44^{high}/ALDH⁺ were analyzed as CSC and CD44^{low}/ALDH⁻ were analyzed as non-CSC.

Wound Healing Assay

UM-SCC-47-luc+ and UM-SCC-103-luc+ were sorted by flow cytometry as described above for CD44 activity. Sorted cells (6×10^4 cells/well) were then placed into 24-well culture plates with 10% DMEM and allowed to grow to 90-100% confluency. A 200ul pipette tip was then used to make 2 parallel wounds per well. Cells were then observed and the area of the wound was measured at time 0, 9, 15, 18, 20, 24, 26 and 28 hours. The area of the open wound was calculated using the NIH ImageJ free software analysis.¹⁹ Percent closure was calculated based on the area of the wound at times of interest divided by area of time 0 for each wound. Time to 100% closure of the wound and mean percent closure at each time point were measured.

Orthotopic Mouse Model

Approvals for the use of the animal model and for collection of cancer specimens were obtained through the University of Michigan's Committee on Use and Care of Animals (UCUCA) and the Institutional Review Board, respectively. Six to eight week old NOD/SCID mice were anesthetized with 30-100mg/kg ketamine and 10 mg/kg xylazine intraperitoneal injections. UM-SCC 47 cells were then injected into the tip of tongue submucosally. The range of cell numbers injected was 500 – 1×10^5 sorted and unsorted cells. The animals were observed for primary tumor growth in the tip of tongue and for regional metastasis using bioluminescence.¹⁰ Evaluation of success tumor placement was determined by bioluminescence (BLI) on post-injection day number 1. Tumor growth at the primary site and metastasis was confirmed by clinical palpation and BLI. Growth of the primary tumors and metastases were monitored weekly for up to 12 weeks by measuring tumor diameters with BLI. A partial glossectomy was performed at 14-28 days after injection to reduce tumor burden and improve the animal's ability to tolerate an oral diet and reduce upper airway obstruction.²⁰ Glossectomy specimens were taken for histologic analysis.

The animals were euthanized and histologic analysis of all tumors was performed to assess gross and histologic evidence of primary tumor growth, to confirm recapitulation of a heterogeneous tumor, confirm BLI regional or pulmonary metastasis, and to evaluate for renewal of CSC based on flow cytometry. All histology slides were reviewed by a Head and Neck pathologist (J.B.M.). Outcomes of interest were rate of tumorigenesis (BLI intensity at weekly intervals), time to regional metastasis (time from injection to first identifiable metastasis by BLI), rate of metastatic growth (BLI intensity of regional metastasis at weekly intervals) and development of distant metastasis (time from injection to identification of distant metastasis by BLI).²¹

Luciferase transfection and Bio-imaging

The cell lines used in this study were transfected with luciferase to provide in-vivo imaging to assess potential metastasis as previously described.^{7-9,14} Mice were anesthetized with isoflurane and placed in the Bioluminescent imaging machine to evaluate primary tumor growth and metastasis based on total number of photons/second.²² To control for background variation, a ratio of tumor region of interest/background control were calculated and recorded to assess for growth.

Primary tumor growth and metastasis in the luciferase-transfected CSC cell lines injected into the mouse model was monitored with weekly BLI. An area around the tumor and metastasis as demonstrated by BLI was observed and a region of interest (ROI) was defined around the tumor luminescence. Total and average photons/second were recorded and standardized to background luminescence to quantify and analyze primary growth and regional metastasis for statistical analysis.

Statistical Analysis

Wound-healing assays were measured based on mean time to 100% closure and percent-closure at each individual time point. Student's t-test was used to calculate differences between means. Outcome measures were BLI intensity (photons/sec), intensity over time (days), and time to metastasis. BLI intensity was measured as average photons/sec over time and log-transformed for comparison. A mixed model approach was used to test differences in intensity and differences over time (days) between the CSC vs. non-CSC groups. Kaplan-Meier survival statistics were used to evaluate time to metastasis between CSC, non-CSC and an unsorted control group. Patients were grouped based on clinical covariates of interest and CD44 expression was calculated. Student's t-test was used to calculate differences between means. Tumor size and CD44 expression were then analyzed as continuous values. Pearson's correlation was then used to calculate correlation coefficient between tumor size and CD44 expression. For survival analysis, CD44 expression was grouped into CD44^{high} and CD44^{low} groups based on percentile rank; 50th percentile was calculated as CD44^{high} and <50th percentile was calculated as CD44^{low}. Kaplan-Meier survival statistics were used to calculate overall survival (time from definitive cancer treatment to death of any cause), disease specific survival (time from definitive treatment to death from disease) and disease free interval (time from definitive treatment to recurrence of disease). P-value of less than 0.05 was considered statistically significant.

Results

In vitro Analysis of CSC Motility

To evaluate CSC mobility, wound healing assays were performed using CD44^{high} versus CD44^{low} cells isolated from UM-SCC-47-luc+ and UM-SCC-103-luc+ (Figure 1A). Figure 1B shows representative photos of the wound healing assay for UM-SCC-47 and UM-SCC-103. Figure 1C summarizes UM-SCC-47 mean percent of wound closure over time. UM-SCC-47 cells sorted for CD44^{high} expressing cells demonstrated significantly greater mean percent wound closure compared to the CD44^{low} expressing cells at 9, 15, 18 and 20 hours (p=0.0001, 0.001, 0.004 and 0.038 respectively). CD44^{high} UM-SCC-103 cells

demonstrated significantly greater mean percentage wound closure compared to CD44^{low} cells at 9, 18 and 20 hours (p=0.012, 0.012, and 0.036 respectively) (Figure 1D). The mean time to closure was significantly shorter in cells sorted for CD44^{high} compared to CD44^{low} sorted cells for both UM-SCC-47 (17.8 hours v. 21 hours; p=0.001) and UM-SCC-103 (20.6 hours v. 25.8 hours; p=0.028) cell lines.

Orthotopic Mouse Model: Tumorigenesis

An orthotopic mouse model was generated based on previous work by Sano and Myers.¹⁸ UM-SCC-47-luc+, 1×10^5 unsorted cells were injected into the tip of the tongue in NOD/SCID mice. (Figure 2A) Tumor growth was measured by luminescence (photons/sec) at the primary site and regional lymph nodes. (Figure 2B) To estimate the relative bioluminescence per cell a known number of UM-SCC-47-luc+ cells were examined for bioluminescence intensity in vitro. Primary tumor and lymph nodes were examined on H&E stained sections to confirm the presence of squamous cell carcinoma. (Figure 2C)

The relative capacity of CSC and non-CSC to generate tumors was compared using the orthotopic mouse model. Tumor cells were sorted to obtain CD44^{high}, CD44^{low}, CD44^{high}/ALDH⁺, CD44^{low}/ALDH⁻ and unsorted control populations. To compare tumorigenic potential of CD44^{high} and CD44^{low} cells, population sizes ranging from 500 – 25,000 UM-SCC-47-luc+ cells/injection were analyzed. The minimum number of cells to produce a tumor was 50 fold lower for CD44^{high} UM-SCC-47-luc+ cells compared to the CD44^{low} cells (500 vs. 25,000). Furthermore primary tumor growth at 28 days was demonstrated in 5/5 mice injected with CD44^{high} cells vs. only 1/4 mice injected with CD44^{low} cells (p=0.047). Similarly, there was a greater capacity for tumor growth in mice injected with 2.5×10^4 CD44^{high}/ALDH⁺ cells compared to CD44^{low}/ALDH⁻ at 28 days post-injection (2/2 v. 0/2 respectively). (Table 1) The rate of tumor take and growth after injecting 2.5×10^4 CD44 sorted cells was significantly higher in the CD44^{high} and CD44^{high}/ALDH⁺ populations compared to CD44^{low} and CD44^{low}/ALDH⁻ population (p=0.0011). Comparison of bioluminescence at individual time points demonstrated a significantly higher levels of luminescence (photons/sec) in the primary tumors generated by CD44^{high} and CD44^{high}/ALDH⁺ cells at days 21, 28, 36 and 43 compared to CD44^{low} and CD44^{low}/ALDH⁻ cells. Collectively, CSC (CD44^{high} and CD44^{high}/ALDH⁺) had significantly greater capacity for tumorigenesis and greater rates of tumor growth compared to non-CSC (CD44^{low} and CD44^{low}/ALDH⁻). (Figure 3A and 3C)

Histologic evaluation of the CD44^{high} and CD44^{high}/ALDH⁺ derived primary tumors demonstrated invasive moderately differentiated squamous cell carcinoma with perineural invasion. (Figure 3B) These results strongly suggest cells expressing high levels of the cancer stem cell marker CD44 and ALDH have greater tumorigenic potential compared to cells expressing CD44^{low} or CD44^{low}/ALDH⁻. High tumorigenic potential in CD44^{high} and CD44^{high}/ALDH⁺ cells further supports CD44 and ALDH as markers for head and neck cancer stem cells.

Orthotopic Mouse Model: Metastasis

Mice injected with 2.5×10^4 CD44^{high} or CD44^{high}/ALDH⁺ cells were assessed for metastatic potential relative to CD44^{low} or CD44^{low}/ALDH⁻ cells. All mice injected with CD44^{high} or CD44^{high}/ALDH⁺ had a significantly shorter metastasis-free interval compared to mice injected with CD44^{low} or CD44^{low}/ALDH⁻ cells (mean time to metastasis 21.6 v. 40 days; $p=0.005$). (Figure 4A) There was significantly greater regional metastatic luminescence in CD44^{high} and CD44^{high}/ALDH⁺ cells injections at 28, 36 and 43 days compared to CD44^{low} and CD44^{low}/ALDH⁻. (Figure 4B and 4C) Histologic analysis of the lymph nodes confirmed the BLI results and the development of spontaneous metastasis of squamous cell carcinoma. (Figure 4D)

A distant metastasis was detected by luminescence in a CD44^{high}/ALDH⁺ mouse that could be kept alive for 71 days post-injection and 38 days post-glossectomy. Bulky lymphadenopathy was seen by luminescence and confirmed by necropsy. Histologic analysis of the regional and distant lung metastasis confirmed spontaneous metastasis of squamous cell carcinoma. (Figure 5E) A comparative CD44^{low}/ALDH⁻ mouse that developed a primary tumor significantly delayed after injection was kept alive for a similar length of time and did not develop distant metastasis.

Patient outcomes and tumor CD44^{high} content

Mean CD44^{high} content of all 40 tumor specimens was 10.8% (range 0% - 84.5%). There was no statistical difference in mean CD44^{high} content between subsites (oral cavity 12.6%, oropharynx 12.9% and larynx 3.2%; $p=0.436$). (Figure 5A) Mean CD44 content in primary tumors relative to regional metastasis, distant metastasis, stage, tumor size, and perineural invasion was evaluated. (Figure 5B-F) Only stage and tumor size were significantly correlated with CD44 content. Advanced stage tumors (AJCC stage III/IV) had significantly elevated CD44 content compared to early stage (AJCC stage I/II) (11.6% versus 1.2%; $p=0.002$). Increased tumor size was associated with elevated CD44 content ($p=0.007$). Tumor specimens from patients with regional metastases had higher CD44^{high} content compared to patient specimens without regional metastases however this was not statistically significant (12% v 9.7%; $p=0.70$). Tumor specimens from patients who had at least 2 years of follow-up were analyzed for association of CD44 enrichment and distant metastases. Patients who developed distant metastases had higher CD44 content compared to patient specimens without distant metastases however this was not statistically significant (10.2% v 4.3%; $p=0.34$). Perineural invasion (PNI) is a known risk factor for regional metastasis. In patients with PNI there were higher levels of CD44^{high} content compared to PNI-negative specimens, however there was no statistical correlation (10.2% and 4.3%; $p=0.32$).

Analysis of patient survival outcomes relative to CD44 content was performed (Figure 5G-H). There was no difference in overall survival, disease-specific survival or disease-free interval ($p=0.961$, $p=0.960$ and $p=0.355$ respectively) among patients with elevated CD44 enrichment compared to those with lower CD44 content.

Discussion

Cancer stem cells (CD44^{high} and CD44^{high}/ALDH+) have significantly increased in-vitro migration and wound healing and in an orthotopic mouse model are more tumorigenic with a greater rate of spontaneous metastasis compared to non-cancer stem cells (CD44^{low} and CD44^{low}/ALDH-). We demonstrate a useful orthotopic mouse model that can be used to study in-vivo tumor growth and spontaneous metastasis using a minimal number of CSC. Additionally, the mouse model has shown the reproducible and reliable ability of CSC to form regional metastasis. These findings suggest CSC (CD44^{high} and CD44^{high}/ALDH+) have a greater capacity for spontaneous regional and distant metastatic spread and growth compared to non-CSC (CD44^{low} and CD44^{low}/ALDH-). This is an important step in defining the role of CSC in metastasis and developing a model for future targeted stem cell therapy. In primary patient tumors, CSC enrichment in primary tumors is significantly associated with increased tumor size and tumor stage, while there were trends for association of CD44^{high} content with regional, distant and perineural invasion. CD44^{high} content was not associated with long-term survival.

Work by others in breast, colorectal, and prostate cancer supports our findings indicating that CSC may play a critical role in tumorigenesis, treatment resistance, and metastasis.^{11-13,23} We initially sought to evaluate in-vitro assays of cell migration via wound healing assay as a proxy to establish CSC as a more aggressive subtype from a wound healing standpoint. Cancer stem cells appear to have a greater rate of wound closure compared to non-CSC for both UM-SCC-47 and UM-SCC-103. To further validate the in-vitro data a more physiologic model was developed. In head and neck cancer, previous work by Davis et al. showed that UM-SCC-47-luc+ (CD44^{high}/ALDH+) cells have a significantly greater ability to colonize the lungs after tail-vein injections than CD44^{high}ALDH-cells.^{8,14} A common concern for the tail vein injection model is that the lung lesions represent tumor seeding or capillary entrapment rather than overt cancer metastasis and invasion. The tip of tongue orthotopic mouse model addresses the ability for CSC recapitulation of heterogeneous tumors with significantly elevated tumorigenicity at the primary site and a significant ability to form spontaneous regional and distant metastasis.

We have shown that cells expressing high levels of CD44 alone or jointly with elevated ALDH activity have a greater ability to form primary tumors and regional metastasis compared to cells lacking these two markers. The development of regional metastasis in the CSC group further strengthens the argument that CSC are an essential regulator and component of metastatic spread. The exact role of CD44 and ALDH in CSC pathophysiology remains unclear. CD44 is a cell surface receptor for the extracellular matrix molecule hyaluronan, with multiple established mechanisms for cancer growth and spread. Specifically, CD44 has been implicated as a cell surface receptor for cell-cell adhesion, cell-matrix adhesion, endothelial attachment and invasion, cell signal transmission and potent mediator for cell proliferation.²⁴ Wang *et al.* were able to show that elevated CD44 was associated with worse survival.²⁴ Over the last several years, its role as a CSC marker has been extensively studied. However, CD44^{high} may not identify all cells with CSC characteristics and has been shown to be a less selective marker of HNCSC than ALDH expression.⁸ If sufficient numbers of CD44^{low} cells such as the experiments in which 2.5 ×

10^4 CD44^{low} non-CSC cells could eventually yield tumor growth and regional metastasis over longer periods of time compared to the CD44^{high} CSC group, the addition of ALDH as a second marker for CSC identification can help demonstrate a more specific marker for CSC ability to form primary tumors and regional metastasis.

ALDH is a well-established marker for normal hematopoietic and nervous system stem cells.²⁵ In addition, ALDH activity has been a significant marker for breast cancer stem cells.¹¹ Work by Clay et al. has shown that ALDH activity is associated with Head and neck cancer stem cells and may be a more specific marker for highly tumorigenic cancer cells.^{8,9} While the in-vitro wound healing assay did not assess CD44^{high}/ALDH⁺ versus CD44^{low}/ALDH⁻, we have shown that when using CD44 and ALDH as concurrent CSC markers, there is a greater ability for primary tumor growth and regional metastasis compared to CD44^{low}/ALDH⁻ injections. Failure to generate regional metastasis in the CD44^{low}/ALDH⁻ group as compared to the CD44^{low} only group suggest that ALDH may be a more specific and necessary marker for identifying CSC and facilitating metastasis. We did not see any gross differences when evaluating CD44^{high} and CD44^{high}/ALDH⁺, however the overall group was small and subgroup analysis would require a larger sample size. However, the exact role that ALDH plays in CSC tumorigenicity and metastasis remains unclear. Future work evaluating CD44^{high}/ALDH⁺ versus CD44^{low}/ALDH⁻ in-vitro may provide a rapid model to further investigate ALDH and CD44 concomitant expression outcomes and potential targets for therapy. Additionally evaluating for differences between CD44^{high} and CD44^{high}/ALDH⁺ in the animal model may provide additional insight into the true effect of ALDH on metastasis.

One of the weaknesses of the study is the potential for non-CSC to form tumors and regional metastasis. The capacity for lymph node metastases for non-CSC were identified and found to be significantly lower compared to CSC. Despite attempts to isolate 100% CSC and 100% non-CSC, the current flow technology does not allow for complete cell expression or marker purity. One can hypothesize that the lymph node growth may represent the impurity of the non-CSC injections. Alternatively, non-CSC may have a low metastatic potential. This question is interesting and requires future study, particularly given the heterogeneous nature of HNSCC.

Grossly, HNSCC is seen as a heterogeneous tumor with varied clinical outcomes. At the cellular level, it is possible that while CSC may have the potential for metastatic spread, the CSC population in an individual tumor is highly heterogeneous and not all CSC are capable of regional or distant metastasis.²⁶ While size and stage were associated with enrichment of CD44^{high} cells, there was no statistical association with metastasis and survival. This suggests that increased enrichment of CD44 cells is associated with tumorigenesis, but not with metastasis and outcome. Limitations of the patient data are the number of patients studied. A larger study may identify associations between CD44 enrichment and metastasis and outcome. CD44 has several variants that are associated with survival outcomes.²⁴ While the antibodies used for flow did not assess CD44-variants, it is very possible that CSC CD44-variant expression mediates metastatic potential. All animals injected with UM-SCC-47 had regional disease, whereas the patient population was not as clear based on CD44 expression. CD44 variants as described by Wang et al. may represent a

vital variable with regards to metastatic capability.²⁴ Future examination of CD44-variant expression within CSC may further delineate metastatic expression signatures in CSC. However, taken in context with the *in vivo* animal study findings that CSC are necessary for metastasis; one could interpret the patient data to support the theory that a limited number of or even a single CSC is capable of forming metastases and that treatment failure or recurrence may be mediated by a small number of residual CSC. (Figure 6A) Metastatic capacity may not be programmed into every CSC and it may be the continued accumulation of mutations or expression alterations that may activate the ability for particular CSC to gain invasive capacity and to form metastasis. Identification of the CSC-metastatic genetic signature may yield the best chance for understanding the CSC-specific mechanisms of metastasis and for targeted treatment. Designing CSC-specific signatures and targets may provide novel insight into diagnostics and potentially novel treatment modalities. (Figure 6B)

Overall, this study demonstrated the essential role CSC have in tumorigenesis and more importantly as a vital component of the development of metastasis. The development of an animal model with the ability to recreate metastatic disease is an important step for understanding the biology of CSC and metastatic disease, but more importantly allows for a model to test potential therapeutics targeting head and neck CSC. Further studies to better define the role that CSC have in tumorigenesis and metastasis and will be critical to developing novel targets for therapy.

Supplementary Material

Refer to Web version on PubMed Central for supplementary material.

Acknowledgments

Grant Support: T32 training grant (T32 DC005356); NIDCR 1 R01-DE019126; University of Michigan SPORE (P50 CA97248)

References

1. Reya T, Morrison SJ, Clarke MF, Weissman IL. Stem cells, cancer, and cancer stem cells. *Nature*. 2001; 414:105–111. [PubMed: 11689955]
2. Jemal A, Siegel R, Xu J, Ward E. Cancer statistics, 2010. *CA Cancer J Clin*. 2010; 60:277–300. [PubMed: 20610543]
3. Genden EM, Ferlito A, Bradley PJ, Rinaldo A, Scully C. Neck disease and distant metastases. *Oral Oncol*. 2003; 39:207–212. [PubMed: 12618192]
4. Kuperman DI, Auethavekiat V, Adkins DR, et al. Squamous cell cancer of the head and neck with distant metastasis at presentation. *Head Neck*. 2010
5. Layland MK, Sessions DG, Lenox J. The influence of lymph node metastasis in the treatment of squamous cell carcinoma of the oral cavity, oropharynx, larynx, and hypopharynx: N0 versus N+ Laryngoscope. 2005; 115:629–639. [PubMed: 15805872]
6. Sano D, Myers JN. Metastasis of squamous cell carcinoma of the oral tongue. *Cancer Metastasis Rev*. 2007; 26:645–662. [PubMed: 17768600]
7. Prince ME, Ailles LE. Cancer stem cells in head and neck squamous cell cancer. *J Clin Oncol*. 2008; 26:2871–2875. [PubMed: 18539966]

8. Prince ME, Sivanandan R, Kaczorowski A, et al. Identification of a subpopulation of cells with cancer stem cell properties in head and neck squamous cell carcinoma. *Proc Natl Acad Sci U S A*. 2007; 104:973–978. [PubMed: 17210912]
9. Clay MR, Tabor M, Owen JH, et al. Single-marker identification of head and neck squamous cell carcinoma cancer stem cells with aldehyde dehydrogenase. *Head Neck*. 2010; 32:1195–1201. [PubMed: 20073073]
10. Charafe-Jauffret E, Ginestier C, Iovino F, et al. Aldehyde dehydrogenase 1-positive cancer stem cells mediate metastasis and poor clinical outcome in inflammatory breast cancer. *Clin Cancer Res*. 2010; 16:45–55. [PubMed: 20028757]
11. Wicha MS. Cancer stem cells and metastasis: lethal seeds. *Clin Cancer Res*. 2006; 12:5606–5607. [PubMed: 17020960]
12. Bao S, Wu Q, McLendon RE, et al. Glioma stem cells promote radioresistance by preferential activation of the DNA damage response. *Nature*. 2006; 444:756–760. [PubMed: 17051156]
13. Vermeulen L, Todaro M, de Sousa Mello F, et al. Single-cell cloning of colon cancer stem cells reveals a multi-lineage differentiation capacity. *Proc Natl Acad Sci U S A*. 2008; 105:13427–13432. [PubMed: 18765800]
14. Davis SJ, Divi V, Owen JH, et al. Metastatic potential of cancer stem cells in head and neck squamous cell carcinoma. *Arch Otolaryngol Head Neck Surg*. 2010; 136:1260–1266. [PubMed: 21173377]
15. Yu CC, Lo WL, Chen YW, et al. Bmi-1 Regulates Snail Expression and Promotes Metastasis Ability in Head and Neck Squamous Cancer-Derived ALDH1 Positive Cells. *J Oncol*. 2011
16. Al-Assar O, Muschel RJ, Mantoni TS, McKenna WG, Brunner TB. Radiation response of cancer stem-like cells from established human cell lines after sorting for surface markers. *Int J Radiat Oncol Biol Phys*. 2009; 75:1216–1225. [PubMed: 19857785]
17. Brenner JC, Graham MP, Kumar B, et al. Genotyping of 73 UM-SCC head and neck squamous cell carcinoma cell lines. *Head Neck*. 2010; 32:417–426. [PubMed: 19760794]
18. Lin CJ, Grandis JR, Carey TE, et al. Head and neck squamous cell carcinoma cell lines: established models and rationale for selection. *Head Neck*. 2007; 29:163–188. [PubMed: 17312569]
19. Schneider CA, Rasband WS, Eliceiri KW. NIH Image to ImageJ: 25 years of image analysis. *Nat Methods*. 2012; 9:671–675. [PubMed: 22930834]
20. Myers JN, Holsinger FC, Jasser SA, Bekele BN, Fidler IJ. An orthotopic nude mouse model of oral tongue squamous cell carcinoma. *Clin Cancer Res*. 2002; 8:293–298. [PubMed: 11801572]
21. Sano D, Myers JN. Xenograft models of head and neck cancers. *Head Neck Oncol*. 2009; 1:32. [PubMed: 19678942]
22. O'Neill K, Lyons SK, Gallagher WM, Curran KM, Byrne AT. Bioluminescent imaging: a critical tool in pre-clinical oncology research. *J Pathol*. 2010; 220:317–327. [PubMed: 19967724]
23. Liu H, Patel MR, Prescher JA, et al. Cancer stem cells from human breast tumors are involved in spontaneous metastases in orthotopic mouse models. *Proc Natl Acad Sci U S A*. 2010; 107:18115–18120. [PubMed: 20921380]
24. Wang SJ, Wong G, de Heer AM, Xia W, Bourguignon LY. CD44 variant isoforms in head and neck squamous cell carcinoma progression. *Laryngoscope*. 2009; 119:1518–1530. [PubMed: 19507218]
25. Corti S, Locatelli F, Papadimitriou D, et al. Identification of a primitive brain-derived neural stem cell population based on aldehyde dehydrogenase activity. *Stem Cells*. 2006; 24:975–985. [PubMed: 16293577]
26. Schneider BL, Kulesz-Martin M. Destructive cycles: the role of genomic instability and adaptation in carcinogenesis. *Carcinogenesis*. 2004; 25:2033–2044. [PubMed: 15180945]

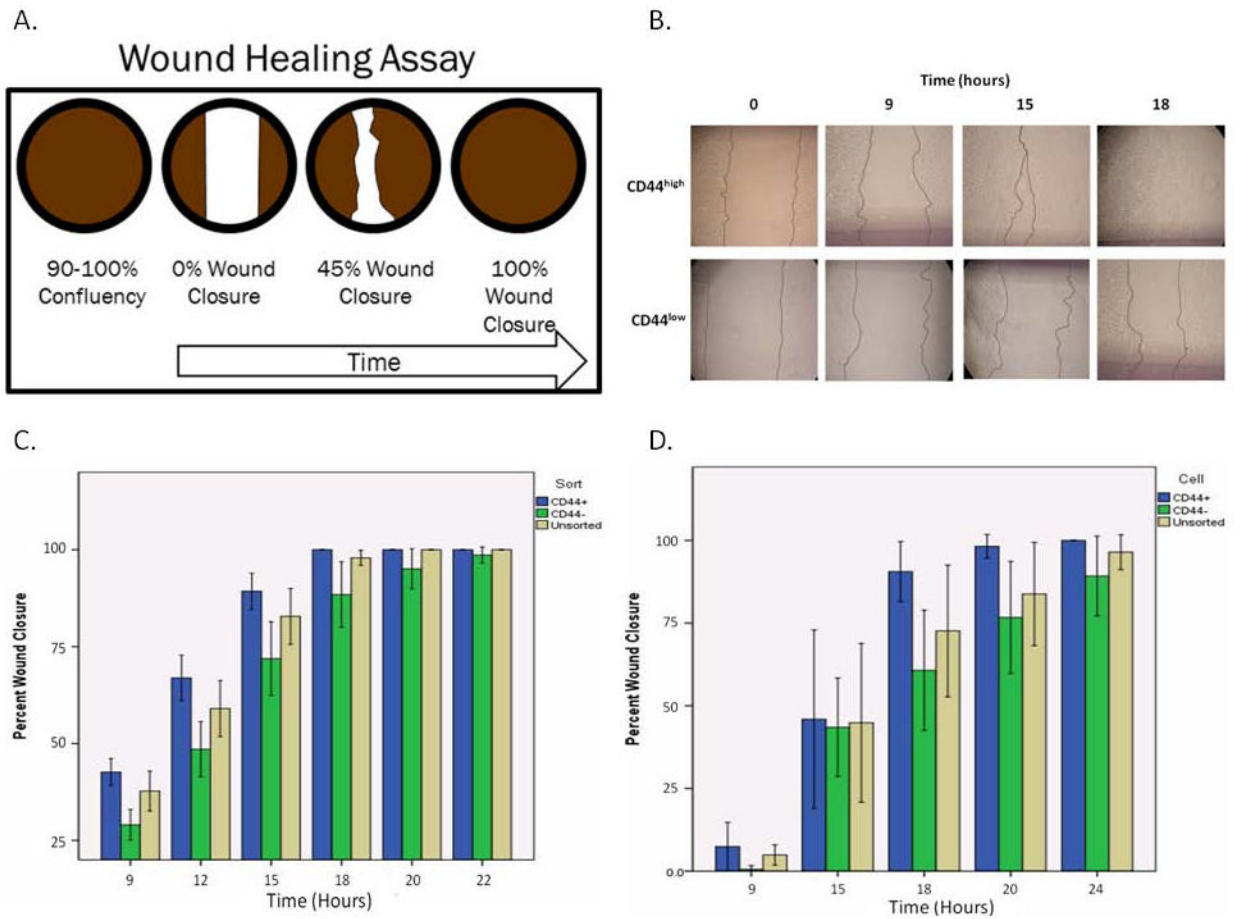


Figure 1. Wound healing assay. (A) Experimental design. (B) Representative wound closure over time between CD44^{high} and CD44^{low} cells. Mean percent wound closure for (C) UM-SCC-47 and (D) UM-SCC-103 cells sorted by CD44. Error bars represent standard error.

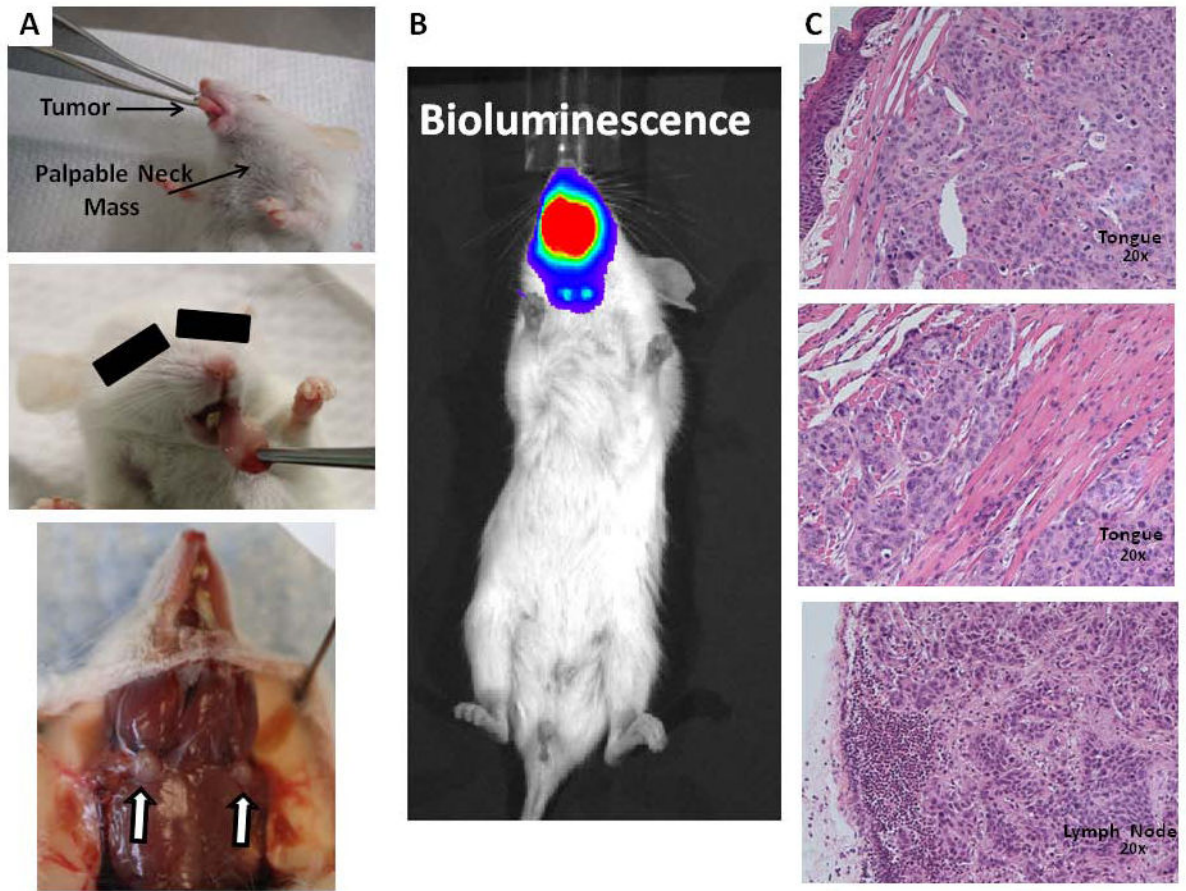


Figure 2.

Validation of orthotopic mouse model. (A) Gross examination of primary tongue growth with palpable neck mass. Post-mortem neck dissection with visible enlarged lymph nodes (White arrows). (B) Bioluminescent imaging (BLI) with high intensity (red) primary tumor and 2 areas of increased intensity around cervical lymph nodes. (C) Hematoxylin and eosin (H&E) staining demonstrates invasive moderately differentiated squamous cell carcinoma with perineural invasion of the primary tumor and metastatic SCC to lymph nodes.

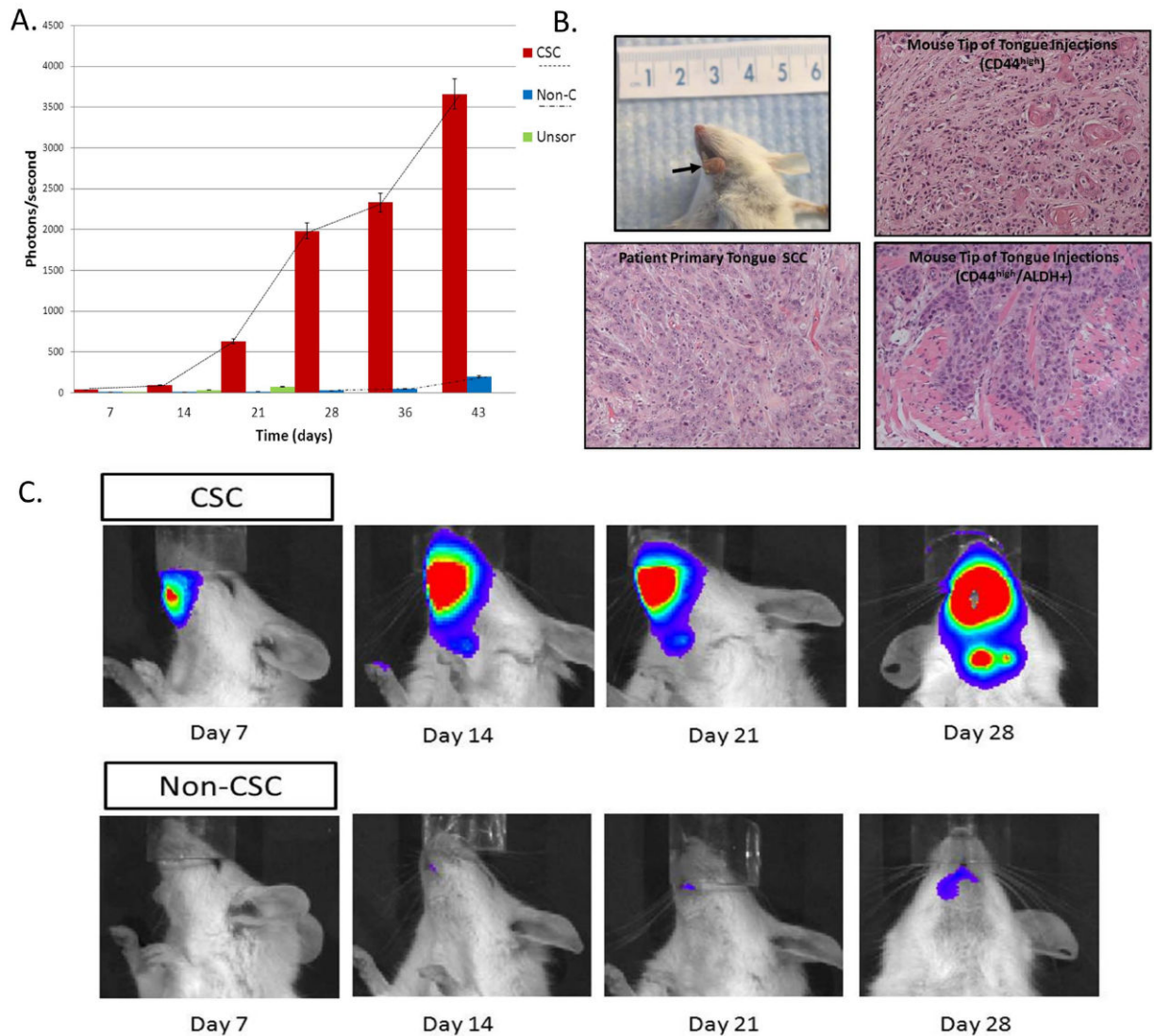


Figure 3. Tumorigenesis: (A) Comparison of bioluminescence (BLI) over time between CSC ([Red] CD44^{high} and CD44^{high}/ALDH⁺), non-CSC ([Blue] CD44^{low} and CD44^{low}/ALDH⁻) and unsorted control [Green]. (B) Gross (arrow) and histologic comparison of CSC-derived squamous cell carcinoma (SCC) compared to primary patient tumor. (C) Representative BLI of CSC and Non-CSC mice at various time points. Error bars represent standard error.

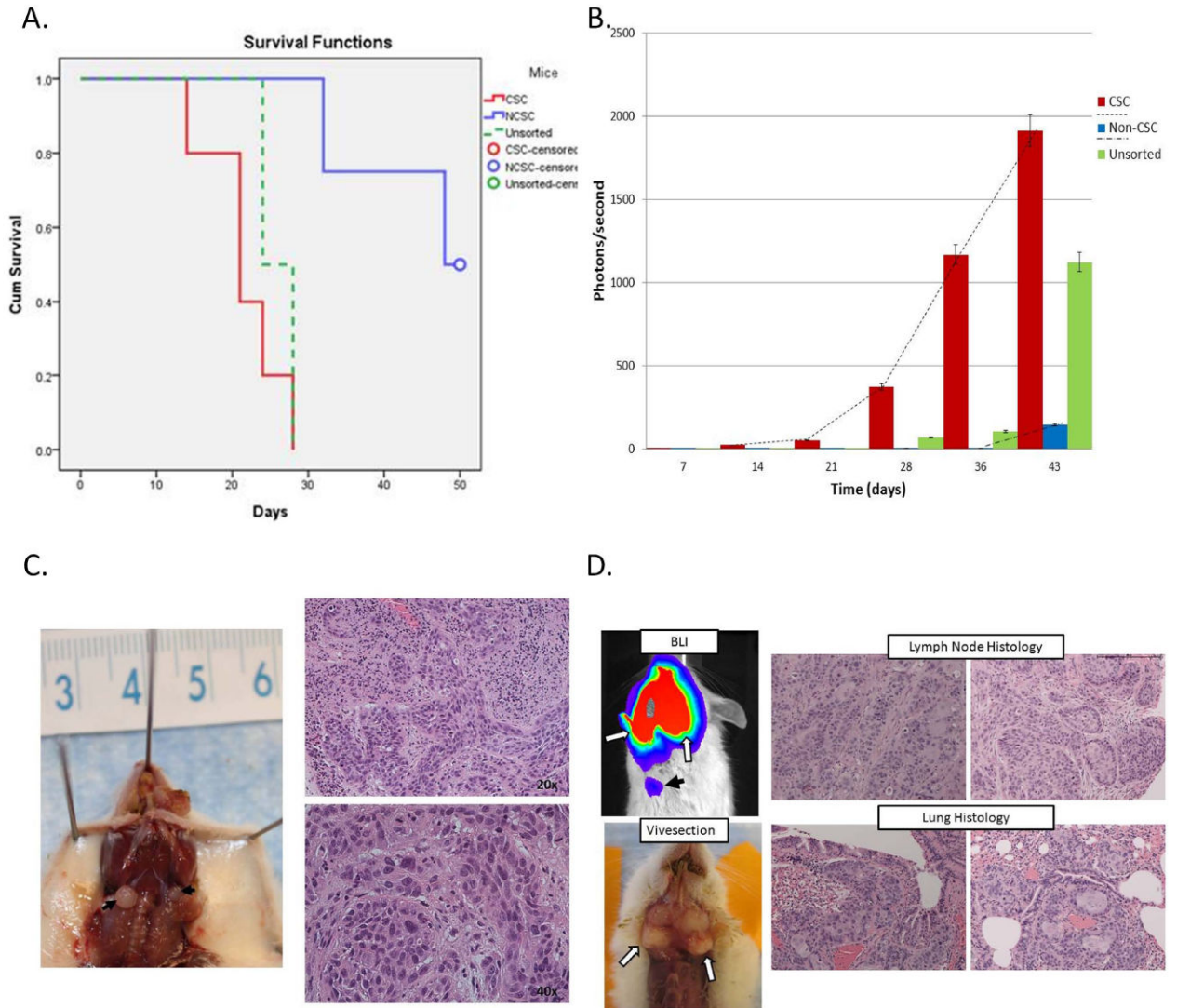


Figure 4. Metastasis: (A) Kaplan-Meier analysis of Time to Regional Metastasis between CSC ([Red] CD44^{high} and CD44^{high}/ALDH⁺), non-CSC ([Blue] CD44^{low} and CD44^{low}/ALDH⁻) and unsorted control [Green]. (B) Comparison of regional metastatic bioluminescence (BLI) over time between CSC ([Red] CD44^{high} and CD44^{high}/ALDH⁺), non-CSC ([Blue] CD44^{low} and CD44^{low}/ALDH⁻) and unsorted control [Green]. (C) Representative BLI of regional metastasis of CSC at various time points. (D) Gross (black arrow head) and histologic comparison of CD44^{high}-derived spontaneous squamous cell carcinoma (SCC) metastasis. (E) Gross (white arrow) and histologic comparison of CD44^{high}/ALDH⁺-derived spontaneous squamous cell carcinoma (SCC) regional (white arrows) and distant metastasis (black arrows).

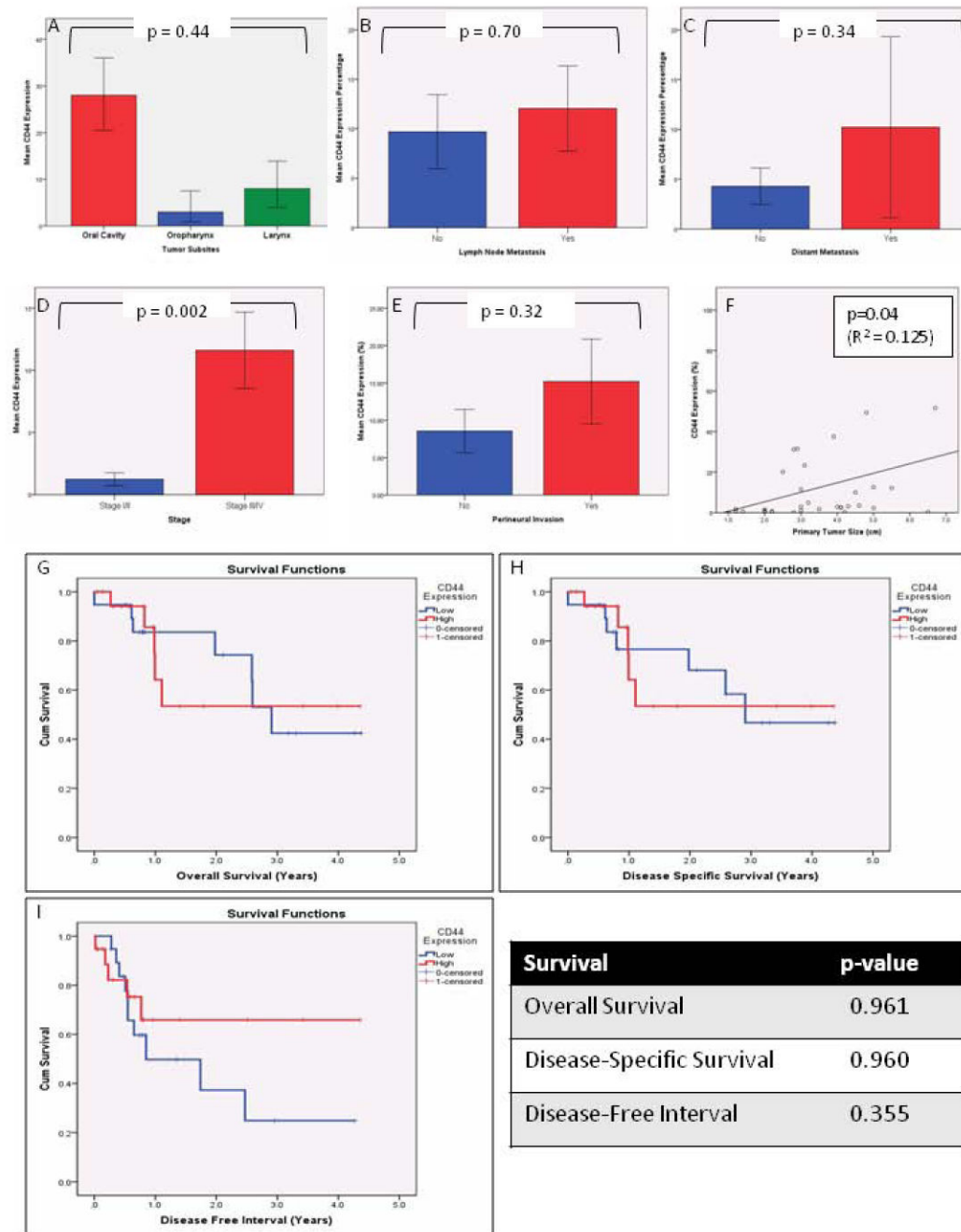


Figure 5. Association of clinical variables and CD44 enrichment in patient derived primary tumor specimens and survival outcome analysis. CD44 enrichment relative to (A) Tumor subsite (oral cavity, oropharynx, and glottis); (B) Lymph node metastasis; (C) Distant metastasis; (D) AJCC Stage (I/II v III/IV); (E) Perineural invasion; (F) Primary tumor size. Outcome measures of tumor specimens with elevated CD44 enrichment (high) versus low CD44 enrichment (low). (G) Overall Survival; (H) Disease-Specific Survival; (I) Disease-Free Interval.

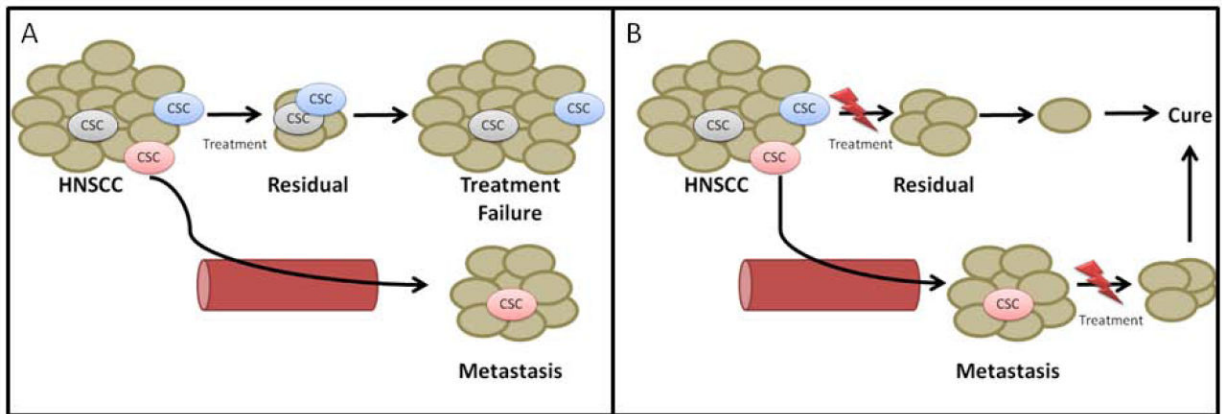


Figure 6. Mechanisms of Treatment Failure and Recurrence. (A) A single CSC may be capable of leaving the primary tumor and spreading to regional and distant sites. Current treatment does not fully target CSC, thus residual, metastatic or resistant CSC are responsible for treatment failure. (B) CSC-specific treatment may lead to improved treatment. (CSC= Cancer stem cell)

Table 1

Tumorigenesis: Number of primary tongue tumors resulting from implantations of CSC (CD44^{high}/ALDH⁺) and non-CSC (CD44^{low}/ALDH⁻) cells for each titration of UIM-SCC-47 cells.

Number of Cells/Injection	CSC	Non-CSC	Control
1×10^5	--	--	2/2
5×10^4	2/2	2/2	1/1
2.5×10^4	5/5	1/4	1/1
1×10^3	1/1	0/1	--
500	1/1	0/1	--

Controls represent unsorted cells. Error bars represent standard error.